Inhibition of glutathione synthesis eliminates the adaptive response of ascitic hepatoma 22 cells to nedaplatin that targets thioredoxin reductase

By: Yijun Wang, Hongjuan Lu, Dongxu Wang, Shengrong Li, Kang Sun, Xiaochun Wan, Ethan Will Taylor, and Jinsong Zhang

Yijun Wang, Hongjuan Lu, Dongxu Wang, Shengrong Li, Kang Sun, Xiaochun Wan, Ethan Will Taylor, Jinsong Zhang. Inhibition of glutathione synthesis eliminates the adaptive response of ascitic hepatoma 22 cells to nedaplatin that targets thioredoxin reductase. *Toxicology and Applied Pharmacology*. Volume 265, Issue 3, 15 December 2012, Pages 342-350. https://doi.org/10.1016/j.taap.2012.09.001

Abstract:

Thioredoxin reductase (TrxR) is a target for cancer therapy and the anticancer mechanism of cisplatin involves TrxR inhibition. We hypothesize that the anticancer drug nedaplatin (NDP), an analogue of cisplatin and a second-generation platinum complex, also targets TrxR. Furthermore, we investigate whether the therapeutic efficacy of NDP can be enhanced by simultaneous modulation of 1) TrxR, *via* NDP, and 2) glutathione (GSH), *via* the GSH synthesis inhibitor buthionine sulfoximine (BSO). Mice bearing ascitic hepatoma 22 (H22) cells were treated with NDP alone or NDP plus BSO. TrxR activity of H22 cells was inhibited by NDP in a dose-dependent manner. A high correlation between the inhibition of TrxR activity at 6 h and the inhibition of ascitic fluid volume at 72 h was established ($r = 0.978$, $p < 0.01$). As an adaptive response, the viable ascitic cancer cells after NDP treatment displayed an enlarged cell phenotype, assembled with several-fold more antioxidant enzymes and GSH-predominant non-protein free thiols. This adaptive response was largely eliminated when BSO was co-administered with NDP, leading to the decimation of the H22 cell population without enhancing renal toxicity, since at this dose, NDP did not inhibit renal TrxR activity. In conclusion, the pharmacological effect of NDP involves TrxR inhibition, and the adaptive response of NDP-treated ascitic H22 cells can be efficiently counteracted by BSO. Simultaneous modulation of TrxR and GSH on ascitic H22 cells using NDP plus BSO greatly enhances therapeutic efficacy as compared with the single modulation of TrxR using NDP alone.

Keywords: Buthionine sulfoximine | Glutathione | Nedaplatin | Thioredoxin reductase

Article:

Abbreviations: ASK1, apoptosis signal-regulated kinase-1; BSA, bovine serumalbumin; BSO, buthionine sulfoximine; BUN, urea nitrogen; CDNB, 1-chloro-2,4-dinitrobenzene; Cr, creatinine; DTNB, 5,5′-dithiobis (2-nitrobenzotic acid); GPx, glutathione peroxidase; GR,

glutathione reductase; GRAN#, granulocytes; GSH, reduced glutathione; GST, glutathione S-transferase; H22, ascitic hepatoma 22 cells; HGB, hemoglobin; i.p., intraperitoneally; LYM#, lymphocytes; NADPH, nicotinamide-adenine dinucleotide phosphate; NDP, nedaplatin; NPFT, nonprotein free thiol; NSCLC, non-small-cell lung carcinoma; SCLC, small cell lung carcinoma; PLT, platelets; RBC, red blood cells; RNR, ribonucleotide reductase; SecTRAPs, seleniumcompromised TrxR-derived apoptotic proteins; SOD, superoxide dismutase; Trx, thioredoxin; TrxR, thioredoxin reductase; WBC, white blood cells.

Introduction

The thioredoxin system, comprising selenocysteine-containing thioredoxin reductase (TrxR), thioredoxin (Trx) and nicotinamide-adenine dinucleotide phosphate (NADPH), participates in a broad range of cellular functions, such as the redox control of apoptosis and proliferation-associated signaling and regulatory proteins (Arnér, 2009). TrxR is over-expressed in many cancer cells, where it incites pro-survival effects and enhances tumor development and resistance to therapeutic modalities (Gromer et al., 2004, Nguyen et al., 2006). TrxR1 knockdown Lewis lung carcinoma cells showed a dramatic reduction in tumor progression and metastasis (Yoo et al., 2006). Several commonly used anticancer drugs including cyclophosphamide, ifosfamide, cisplatin and oxaliplatin (Wang et al., 2007, Wang et al., 2008, Witte et al., 2005, Zhang et al., 2008) inactivate TrxR activity, thus adding to the cytotoxic potential of these agents. The selenocysteine-dependent TrxR enzyme has emerged as an important molecular target for anticancer drug development (Cai et al., 2012b, Pennington et al., 2007, Tonissen and Di Trapani, 2009).

Glutathione (GSH), a predominant nonprotein free thiol (NPFT) molecule found in cells at millimolar concentrations, plays a crucial role in cell defense mechanisms by acting as an antioxidant or conjugating with toxic electrophiles (Davis et al., 2001, Lu et al., 2007). The sensitivity of cancer cell lines to chemotherapy is inversely correlated with their GSH content (Andringa et al., 2006, Dai et al., 1999, Meurette et al., 2005, Wu et al., 2004). A positive correlation between elevation of intracellular GSH levels and resistance to platinum or alkylating agents has been established (Biroccio et al., 2004, Dai et al., 1999, Troyano et al., 2001). In cultured MCF-7 cells, GSH depletion by buthionine sulfoximine (BSO), an inhibitor of GSH synthesis, markedly potentiates the cytotoxicity of arsenic trioxide, a TrxR inhibitor. Accordingly, the simultaneous modulation of TrxR and GSH is considered as a powerful strategy for cancer therapy (Lu et al., 2007).

Cis-diammine-glycolate-O,O′-platinum II (nedaplatin, referred to as NDP) is a second-generation platinum complex developed and approved in Japan (Ogawa, 1996, Sasaki et al., 1991). As an analogue of cisplatin, NDP has a novel ring structure in which glycolate is bound to platinum by a bidentate ligand (Alberto et al., 2009). NDP is ten-fold more water soluble than cisplatin (Vermorken, 2001). NDP causes significantly less nausea, vomiting and nephrotoxicity than cisplatin and thus can be given without hydration (Desoize and Madoulet, 2002, Kawai et al., 2005, Ogawa, 1996, Sasaki et al., 1991, Vermorken, 2001). The dose-limiting toxicity of NDP is myelosuppression, in particular thrombocytopenia (Desoize and Madoulet, 2002, Kawai et al., 2005, Ogawa, 1996, Sasaki et al., 1991, Vermorken, 2001). The anticancer mechanism of NDP involves the formation of reactive platinum complexes that bind to nucleophilic groups in

DNA, leading to intrastrand and interstrand DNA cross-links and cellular apoptosis (Alberto et al., 2009). Preclinical and clinical studies have demonstrated that nedaplatin has anticancer activities equivalent to that of cisplatin (Desoize and Madoulet, 2002, Ogawa, 1996, Sasaki et al., 1991, Vermorken, 2001). Since its approval in 1995, NDP has been used in the treatment of testicular tumors, small cell lung carcinoma (SCLC), non-small-cell lung carcinoma (NSCLC), esophageal cancer, bladder cancer, ovarian and cervical cancers, and head and neck tumors (Desoize and Madoulet, 2002, Kawai et al., 2005, Koshiyama et al., 2005, Monk et al., 1998, Ogawa, 1996, Vermorken, 2001).

We have reported previously that cisplatin inactivated TrxR activity in ascitic hepatoma 22 (H22) cells in mice (Zhang et al., 2008). The current work investigated whether NDP targets TrxR of cancer cells *in vivo*. We found that the TrxR activity of ascitic H22 cells in mice could be inhibited by NDP in dose-dependent fashion, and the inhibition of TrxR activity was highly correlated with the inhibition of ascitic fluid volume. As an adaptive response, the viable ascitic H22 cells after NDP treatment displayed an enlarged cell phenotype, equipped with 2 to 5-fold more of various antioxidant enzymes and GSH-predominant NPFT. This adaptive response could be almost fully counteracted by BSO, greatly enhancing the cytotoxicity of NDP without generating renal toxicity, since at the dose used, NDP did not inhibit renal TrxR activity.

Materials and methods

Chemicals and drugs

BSO, NADPH, HEPES, insulin, 5,5′-dithiobis (2-nitrobenzotic acid) (DTNB), Trx (*E. coli*), guanidine hydrochloride, reduced GSH, bovine serum albumin (BSA), 1-chloro-2,4-dinitrobenzene (CDNB), RNase A and propidium iodide were all purchased from Sigma (St. Louis, MO, USA). NDP was purchased from Nanjing Tung Chit Pharmaceutical Co., Ltd., PR China. Other chemicals were of the highest grade available.

Animals

Healthy male Kunming mice (body weight 20–22 g) and their diet were purchased from Shanghai SLAC Laboratory Animal Co. Ltd., PR China. The mice were housed in plastic cages in a room with controlled temperature (22 ± 1 °C) and humidity (50 ± 10%) and 12 h light/dark cycle. The mice were allowed to obtain food and water *ad libitum*.

Tumor cell inoculation

H22 murine carcinoma cells were obtained from the Cell Bank of the Chinese Academy of Sciences (Shanghai, China). In brief, viable cells in ascitic fluid were counted using trypan blue dye exclusion. The concentration of cells in ascitic fluid was adjusted to 100×10^6 cells/mL using saline, then 0.2 mL was intraperitoneally (i.p.) injected into the peritoneal cavity of mice; this procedure was carried out once weekly.

Animal treatments

All experiments involving mice were performed in strict compliance with the ethical guidelines issued by the Anhui Agricultural University.

In the first set of experiments, to investigate the dose effect of NDP on cellular antioxidant parameters and ascitic fluid volume, 48 mice were randomly divided into 4 groups of 12. Seventy-two hours after cell inoculation at a level of 20 million cells per mouse, group I was i.p. injected with saline as control, and groups II–IV were i.p. injected with NDP at the doses of 15, 25 and 35 mg/kg, respectively. Six mice in each group were euthanized by cervical dislocation at 6 h, and the rest were euthanized at 72 h after NDP treatment. Ascitic fluid was collected directly or with the aid of a known volume of ice cold saline if necessary and centrifuged to obtain H22 cells.

In the second set of experiments, to observe the effects of NDP on cell cycle, proliferation, morphology and cellular antioxidant inclusion, 24 mice were randomly divided into 2 groups of 12. Seventy-two hours after cell inoculation at a level of 20 million cells per mouse, group I was i.p. injected with saline as control, and group II was i.p. injected with NDP at a dose of 25 mg/kg. Six mice in each group were euthanized by cervical dislocation at 6 h, and the rest were euthanized at 72 h after NDP treatment. Ascitic fluid was collected directly or with the aid of a known volume of ice cold saline if necessary and centrifuged to obtain H22 cells.

In the third set of experiments, to inspect the potential toxicity of BSO and its effects on NPFT levels as well as H22 cell proliferation, twenty-four mice were randomly divided into 2 groups of 12. Seventy-two hours after cell inoculation at a level of 20 million cells per mouse, group I was i.p. injected with saline as control, and group II was i.p. injected with BSO at a dose of 500 mg/kg. Six mice in each group were euthanized by cervical dislocation at 6 h, and the rest were euthanized at 72 h after BSO treatment. Ascitic fluid samples were collected to obtain H22 cells, and renal tissues were dissected.

In the fourth set of experiments, to elucidate the effect of BSO on NDP cytotoxicity, 36 mice were randomly divided into 3 groups of 12. Seventy-two hours after cell inoculation at a level of 20 million cells per mouse, group I was i.p. injected with saline as control, groups II and III were i.p. injected with NDP at a dose of 25 mg/kg, and group III was simultaneously i.p. injected with BSO at a dose of 500 mg/kg. Six mice in each group were euthanized by cervical dislocation at 6 h, and the rest were euthanized at 72 h after NDP treatment. Ascitic fluid was collected directly or with the aid of a known volume of ice cold saline if necessary and centrifuged to obtain H22 cells.

In the fifth set of experiments, to address the impact of BSO on NDP toxicity, 42 mice were randomly divided into 3 groups of 14. Group I was i.p. injected with saline as control, groups II and III were i.p. injected with NDP at a dose of 25 mg/kg, and group III was simultaneously i.p. injected with BSO at a dose of 500 mg/kg. Six mice in each group were euthanized by cervical dislocation at 6 h after NDP treatment to dissect kidney tissues; the rest were euthanized at 72 h after NDP treatment to obtain blood samples and kidney tissues.

Sample preparation and biochemical parameters

H22 cells were homogenized in ice cold 0.15 M PBS (pH 7.2) with 1 mM $EDTANa_2$ by ultrasonication for 30 min in an ice bath. Kidney tissues were homogenized in a glass homogenizer with the above-mentioned PBS (1:9, w/v). Blood samples collected in EDTA-coated tubes were subjected to hematological evaluation including white blood cells (WBC), red blood cells (RBC), hemoglobin (HGB), platelets (PLT), lymphocytes (LYM#), and granulocytes (GRAN#) by using an auto analyzer. Blood samples collected in EDTA-coated tubes were centrifuged to obtain plasma for measuring urea nitrogen (BUN) and creatinine (Cr) levels by using commercial kits.

For the NPFT assay, immediately after homogenization, an aliquot of homogenate was taken out to mix with trichloroacetic acid (20%, w/v), at the volume ratio of 10:1. This procedure has been confirmed to be able to precipitate all proteins in the homogenate and make GSH in the homogenate stable at 4 °C for at least 2 h (Wang et al., 2008). The trichloroacetic acid-treated homogenate was centrifuged at 10,000 *g* and 4 °C for 5 min. Within 2 h after centrifugation, the supernatant was mixed with DTNB (20 mg/mL in 0.2 M PBS, pH 8.0) and absorbance was read at 412 nm (Wang et al., 2008). Protein levels were determined by the Bradford dye-binding assay with BSA as standard. Since the cell dimension increased substantially and cellular soluble protein level accordingly increased after NDP treatment, activity per million cells rather than per mass of protein was more appropriate for use as a basis for normalization. Thus NPFT level was expressed as nmol GSH/million cells (Barranco et al., 1990, Hunter et al., 1987, Lee et al., 1989).

For antioxidant enzyme assays, the remaining homogenate was centrifuged at 15,000 *g* and 4 °C for 15 min. The supernatants were used for activity determinations, including TrxR, glutathione peroxidase (GPx), glutathione S-transferase (GST), glutathione reductase (GR) and superoxide dismutase (SOD).

TrxR activity assay

TrxR activity was measured based on the method of Holmgren and Björnstedt (1995) with some modifications. A stock mixture was composed of HEPES buffer (1.0 M, pH 7.6), NADPH (40 mg/mL), EDTA (0.2 M) and insulin (10 mg/mL) in the volume ratio of 5:1:1:12.5. In a 96-well plate, 7 μL stock mixture, 3 μL Trx (2 mg/mL), 40 μL HEPES (50 mM, pH 7.6) and 20 μL sample (with 20–30 μg protein) were added to each well. The enzymatic reaction was maintained at 37 °C for 20 min, and then terminated by adding 240 μL stop solution (6 M guanidine hydrochloride, 0.2 mg/mL DTNB, 0.2 M Tris, pH 8.0). Each sample contained a non-enzymatic reaction as the control. The non-enzymatic reaction included all components except Trx, which was substituted by the same volume of saline. The 96-well plates were read at 412 nm. The absorbance of the control was subtracted from the absorbance of the sample. A background control, which was the subtraction of absorbance with and without Trx in the absence of tissue homogenate, was further subtracted from all samples. TrxR activity unit was defined as nmol of NADPH oxidized/min and TrxR activity was expressed as U/million cells.

Other antioxidant enzyme assays

GPx was assayed by the method of Rotruck et al. (1973). Units of GPx activity were calculated in terms of μmols of GSH oxidized/min/million cells. GST activity was chemically determined by using 1-chloro-2,4-dinitrobenzene (CDNB). Units of GST activity were calculated in terms of nmol CDNB changed/min/million cells (Habig et al., 1974). GR activity was assessed by the method of Carlberg and Mannervik (Carlberg and Mannervik, 1985); units of GR activity were calculated in terms of nmols of NADPH oxidized/min, and GR activity was expressed as U/million cells. SOD activity was assayed by using the system of xanthine–xanthine oxidase and nitroblue tetrazolium. Units of SOD activity were defined as inhibition of 50% nitroblue tetrazolium reduction rate/million cells (Sun et al., 1988).

Cell cycle analysis

H22 cells (5×10^6) were washed twice with PBS and fixed in 70% ice cold ethanol at − 20 °C until analysis. The fixed cells were then washed twice with PBS to remove ethanol, incubated with 100 μL 1 mg/mL of RNase A at 37 °C for 30 min. Then, 400 μL 50 μg/mL of propidium iodide was added to the incubated cells for another 30 min at 4 °C in the dark, with gentle shakes. Subsequently, cell cycle phase distribution of nuclear DNA was assayed by flow cytometry (FACS Calibur) (Wang et al., 2008). The fluorescence detector was equipped with 488 nm argon laser light source and 623 nm band pass filter (linear scale) using Cell Quest software (Becton Dickinson). A total of 10,000 events were collected and the analysis of the flow cytometric data was performed with ModFit software. For each sample, data were acquired through two gates, FSC *versus* SSC and FL2W *versus* FL2A, to reduce debris and other contamination (Wang et al., 2008).

Cell morphology and histopathological observation

Cells were stained with hematoxylin and eosin (H&E) and observed under an optical microscope. Kidneys tissues were fixed in 10% neutral buffered formalin solution and embedded into molten paraffin wax. Tissue sections of 5 μm thickness were stained with H&E and observed under an optical microscope by a pathology expert who was blind to the treatments.

Statistical analysis

Data are presented as mean ± SEM. The differences between groups were evaluated by one way ANOVA post hoc Tukey's or Dunnett's multiple comparison tests using GraphPad Software (Prism version 5, San Diego, California, USA). A p value of less than 0.05 was considered statistically significant. During ANOVA analysis, when Bartlett's test for equal variances showed that the variances were significantly different ($p < 0.05$), the differences between groups were evaluated by Dunnett's multiple comparison test. Otherwise, the differences between groups were evaluated using Tukey's multiple comparison tests.

Results

Dose effect of NDP on TrxR and ascitic fluid volume

After a bolus dose of NDP (15, 25 or 35 mg/kg) was administered, at 6 h, TrxR activity significantly decreased in a dose-dependent manner, by 31%, 49% and 77%, respectively, in comparison with the control (Fig. 1A). However, NPFT level and the activities of other antioxidant enzymes (GR, GPx, GST and SOD) had no significant variation. At 72 h, ascitic fluid volume dose-dependently decreased by 39%, 56% and 71%, compared with the control (Fig. 1B). The TrxR inhibition at 6 h was highly correlated with the inhibition of ascitic fluid production at 72 h (r = 0.978 and $p < 0.01$, Fig. 1C).

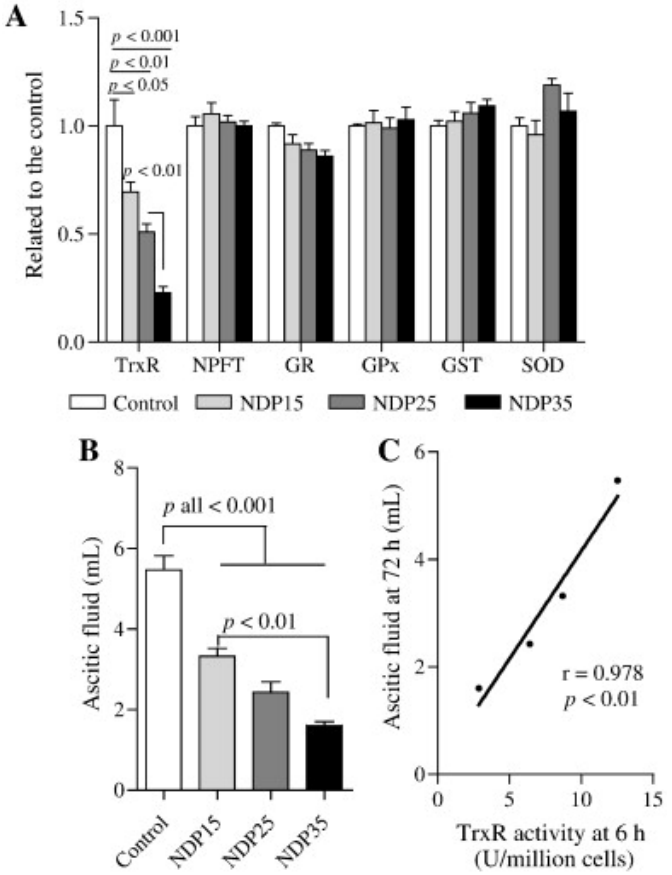

Figure 1. Dose effect of NDP on TrxR activity and ascitic fluid volume. Mice were i.p. injected with either saline or NDP at 15, 25 or 35 mg/kg. Half of the mice in each group were euthanized at 6 h, and the rest were euthanized at 72 h. (A) Antioxidant parameters at 6 h. The basal NPFT level was 1.6 nmol/million cells. The basal activities of TrxR, GR, GPx, GST and SOD were 0.18 U/million cells, 3.3 U/million cells, 7.0 U/million cells, 3.2 U/million cells and 20.1 U/million cells, respectively. (B) Volume of ascitic fluid at 72 h. (C) The correlation between ascitic fluid volume and TrxR activity.

Effects of NDP on cell cycle, proliferation, morphology and antioxidant parameters

NDP treatment at the dose of 25 mg/kg for 72 h caused cell cycle arrest at G2/M phase (Fig. 2A). Such cells displayed an enlarged phenotype (Fig. 2B), appeared to proliferate rather slowly (Fig. 3A), and possessed approximately 3 times as much soluble protein as compared with the control (Fig. 3B). Since soluble protein itself was a variable, it was not appropriate to use it as a basis for normalization. We thus used per million cells as a normalization basis for antioxidant parameters in the present study. Accordingly, TrxR activity and NPFT level in the enlarged cells were increased 3 and 5-fold relative to the control, respectively (Figs. 3C, D).

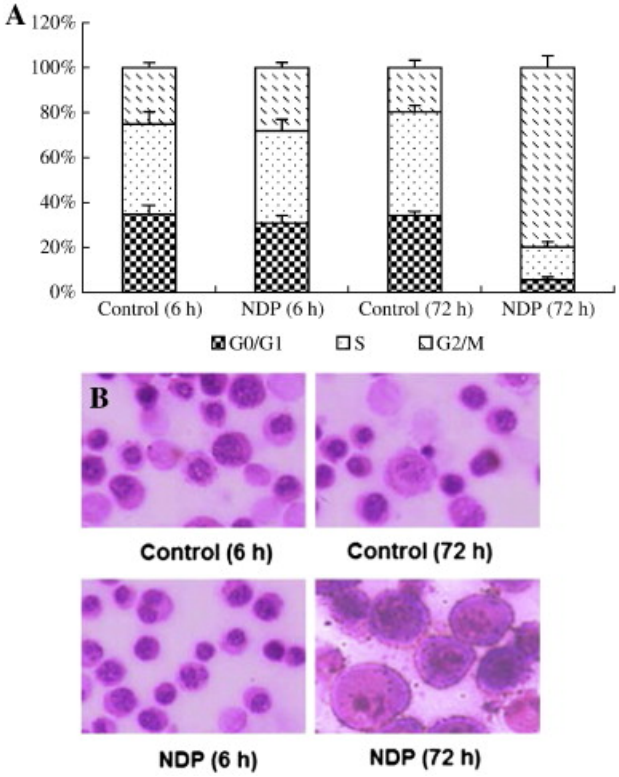

Figure 2. (A) Effect of NDP on cell cycle distribution. (B) Effect of NDP on cellular morphology (H&E, × 200). Mice were i.p. injected with saline or NDP 25 mg/kg. Half of the mice in each group were euthanized at 6 h, and the rest were euthanized at 72 h.

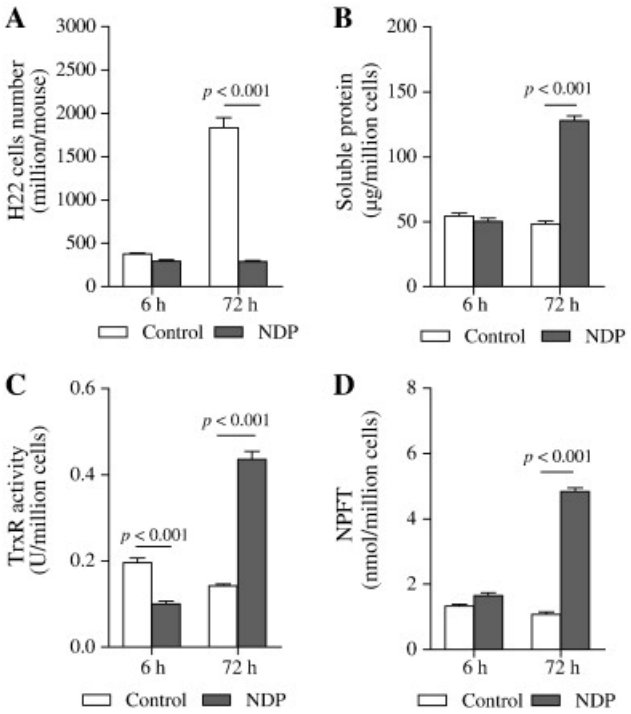

Figure 3. Effects of NDP on cell proliferation and cellular antioxidant inclusion. Mice were i.p. injected with saline or NDP 25 mg/kg. Half of the mice in each group were euthanized at 6 h, and the rest were euthanized at 72 h. (A) H22 cell number. (B) Soluble protein. (C) TrxR activity. (D) NPFT level.

Impacts of BSO on NPFT levels and TrxR activity of H22 cells and renal tissues

BSO treatment at the dose of 500 mg/kg for 6 h and 72 h did not alter TrxR activity in H22 cells and renal tissues (data not shown). As expected, it significantly suppressed NPFT levels in H22 cells and renal tissues by the magnitudes of 60% to 70% at either 6 h or 72 h. The BSO treatment neither suppressed H22 cell proliferation (data not shown) nor generated perceived toxic symptoms including growth suppression in the tested mice. Therefore, the BSO level used generated a specific effect of suppressing NPFT levels without initiating cytotoxicity and host toxicity.

Impact of BSO on NDP cytotoxicity

Consistent with the above results (Fig. 1A), at 6 h, 25 mg/kg NDP alone significantly suppressed TrxR activity by 50% (Fig. 4A) and had no significant impact on NPFT level (Fig. 4B). The co-administration of BSO did not enhance TrxR activity inhibition as compared to treatment with NDP alone (Fig. 4A), but NDP in combination with BSO resulted in significant inhibition of both TrxR activity and NPFT level at 6 h (Figs. 4A, B).

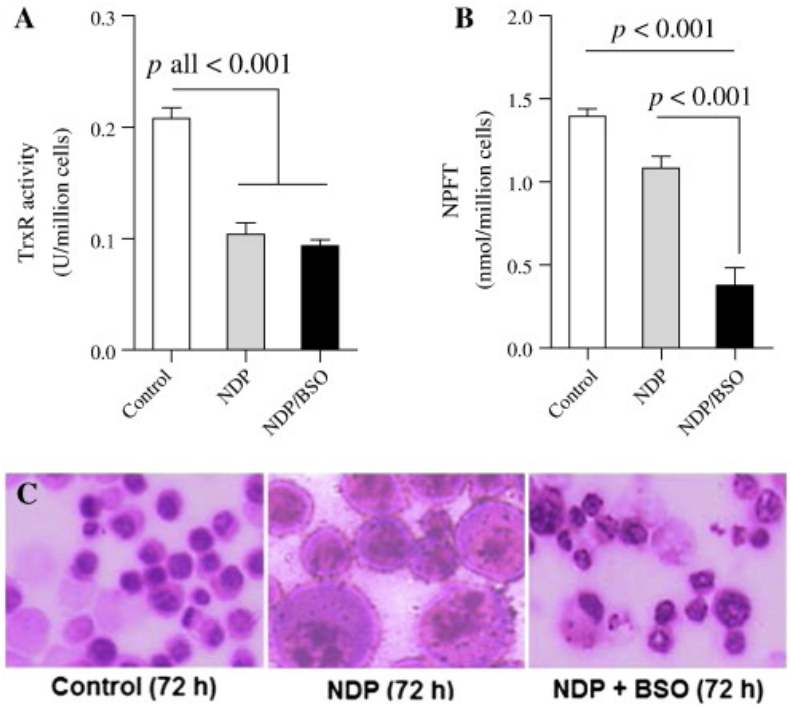

Figure 4. Impact of BSO on the effect of NDP. Mice were i.p. injected with either saline, 25 mg/kg NDP or 25 mg/kg NDP plus 500 mg/kg BSO. Half of the mice in each group were euthanized at 6 h, and the rest were euthanized at 72 h. (A) TrxR activity at 6 h. (B) NPFT level at 6 h. (C) Effect of BSO on NDP-induced morphology enlargement at 72 h (H&E, × 200).

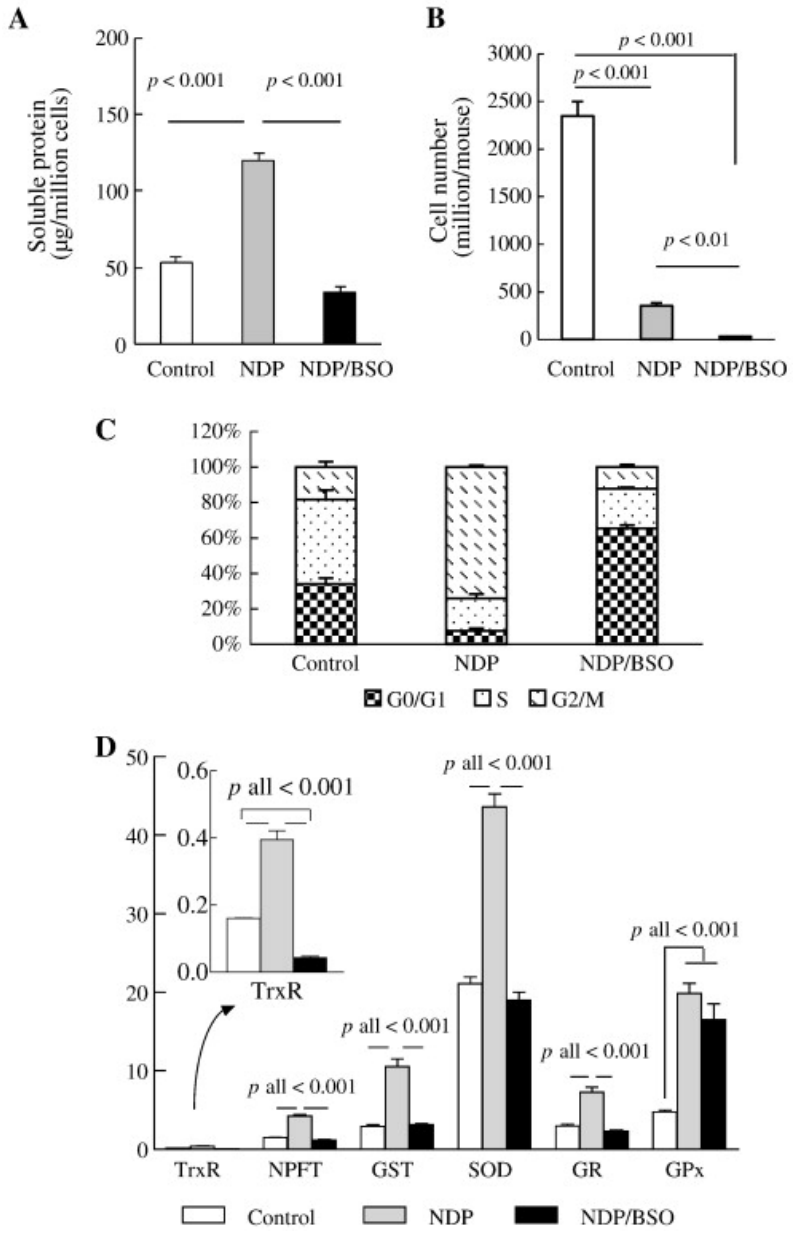

Figure 5. Impact of BSO on the effect of NDP. Mice were i.p. injected with either saline, 25 mg/kg NDP or 25 mg/kg NDP plus 500 mg/kg BSO and were euthanized at 72 h. (A) Soluble protein. (B) Cell number. (C) Cell cycle distribution. (D) Antioxidant parameters. The basal NPFT level was 1.5 nmol/million cells. The basal activities of TrxR, GST, SOD, GR and GPx were 0.16 U/million cells, 2.9 U/million cells, 21.1 U/million cells, 3.0 U/million cells and 4.8 U/million cells, respectively.

Consistent with the above observations (Fig. 2, Fig. 3), at 72 h, 25 mg/kg NDP alone caused enlargement of cellular volume (Fig. 4C), elevation of soluble protein level (Fig. 5A), proliferation inhibition (Fig. 5B), and cell cycle arrest at G2/M phase (Fig. 5C). The co-administration of BSO fully prevented NDP-induced cell enlargement and protein elevation (Figs. 4C, 5A), powerfully enhanced the cytotoxic potential of NDP (Fig. 5B), and shifted cell cycle arrest to G0/G1 phase (Fig. 5C). On the basis of per million cells, TrxR activity in NDP-treated enlarged cells was increased 2.5-fold relative to the control. In contrast, NDP and BSO co-treatment decreased TrxR activity by 73% (Fig. 5D). Furthermore, the NPFT level in NDP-

treated cells was increased 3-fold relative to the control, while NPFT level in NDP and BSO co-treated cells remained close to the control (Fig. 5D). Similarly, other antioxidant enzymes increased after treatment with NDP alone, and were suppressed to the control level by BSO, except for GPx (Fig. 5D). On the other hand, mice were able to tolerate very well both the NDP monotherapy treatment and the combination of BSO and NDP; no perceived toxic symptoms were observed during the time frame of the experiment.

Impact of BSO on hematological and renal toxicities of NDP

At 6 h, 25 mg/kg NDP alone did not significantly inhibit renal TrxR activity and alter renal NPFT level as compared with the control (Figs. 6A, B). The co-administration of BSO powerfully suppressed renal NPFT level (Fig. 6B), and, unlike the profile seen in H22 cells, BSO noticeably did not simultaneously generate significant inhibition of both renal TrxR activity and renal NPFT levels at 6 h (Figs. 6A, B).

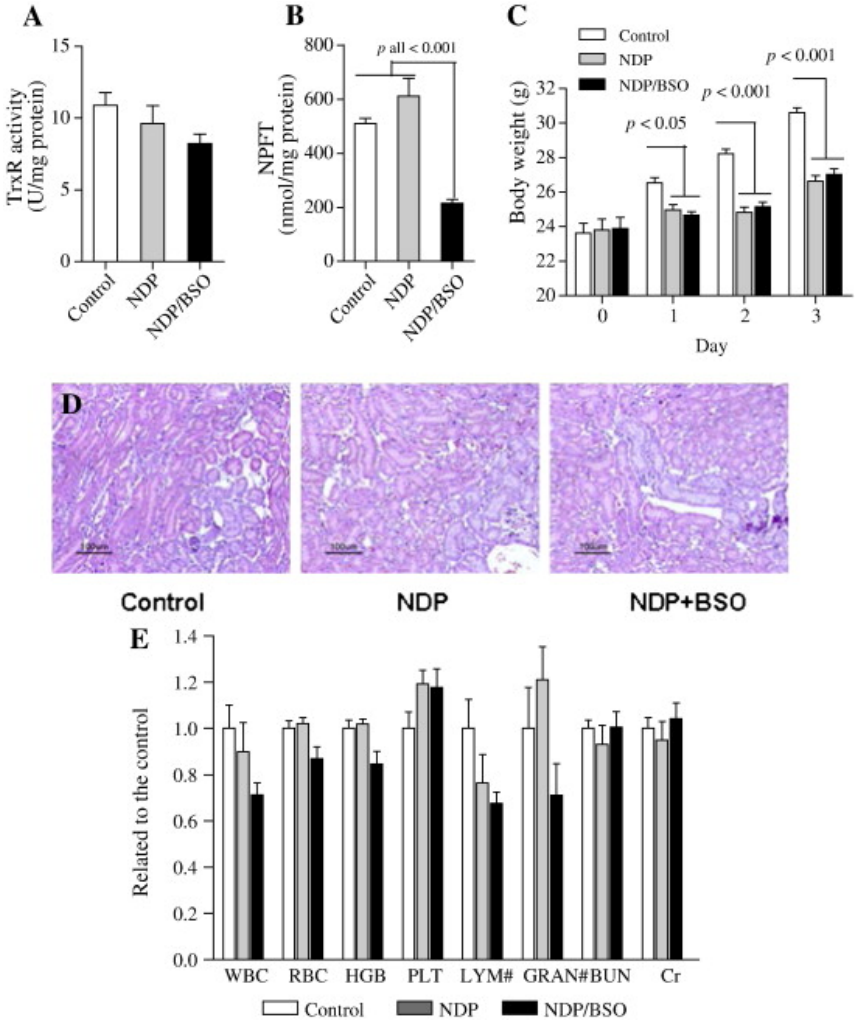

Figure 6. Toxicological investigations of the addition of BSO to NDP treatment. Mice were i.p. injected with either saline, 25 mg/kg NDP, or 25 mg/kg NDP plus 500 mg/kg BSO. Six mice in each group were euthanized at 6 h, and the rest were euthanized at 72 h after NDP treatment. (A) Renal NPFT levels at 6 h. (B) Renal TrxR activity at 6 h. (C) Gain in body weight. (D) Histopathological observation of kidney at 72 h (H&E, × 200). (E) Hematological and plasma biochemical parameters at 72 h.

As shown in Fig. 6C, mice in the control group grew daily, whereas 25 mg/kg NDP alone significantly suppressed the gain of body weight, indicating a toxic response. However, the co-administration of BSO did not enhance the growth suppression compared to treatment with NDP alone. At 72 h, neither NDP alone nor the combination of NDP and BSO altered renal structures (Fig. 6D), hematological parameters, or plasma BUN and Cr levels (Fig. 6E).

Discussion

As an electrophile, NDP should be able to react with nucleophiles. Mammalian TrxR has a redox-active site (Cys496/Sec497) within the C-terminal tetrapeptide motif (Gladyshev et al., 1996). The pKα value of Sec497 is 5.2 (Nordberg and Arnér, 2001), making Sec497 in the TrxR molecule present in the form of $–Se^-$ at physiological pH. Given that $–Se^-$ possesses a stronger nucleophilicity and lower pKa value compared with Cys496, TrxR has the propensity to be attacked by electrophiles, so it is conceivable that TrxR acts as a molecular target for NDP. Inactivation of TrxR by NDP may impede reduction of oxidized Trx and induce apoptosis *via* activating apoptosis signal-regulated kinase-1 (ASK1) (Saitoh et al., 1998). Since selenium compromised TrxR-derived apoptotic proteins (SecTRAPs) could act as potent killers *via* inducing apoptotic cell death (Anestål and Arnér, 2003, Anestål et al., 2008, Cai et al., 2012a), NDP-modified TrxR may further add to the cytotoxic potential of NDP. In the present study, at 6 h after NDP treatment, TrxR activity in ascitic H22 cells was inhibited (Fig. 1A), while GSH-predominant NPFT and other antioxidant enzymes had no significant changes (p all > 0.05, Fig. 1A). NDP caused dose-dependent inhibition of TrxR activity at 6 h (Fig. 1A) and dose-dependent reduction of ascitic fluid volume at 72 h (Fig. 1B); moreover, the former was well correlated with the latter in a positive linear pattern (r = 0.978, Fig. 1C). These results provide *in vivo* evidence that the pharmacological effect of NDP is associated with the inhibition of TrxR activity. As to the selection of cancer cell line *in vivo*, one of the purposes of this study is the demonstration that BSO is able to eliminate NDP-induced drug-resistance. Establishing a NDP-resistant cell model *in vivo* is more likely to succeed using a hepatoma cell line, since hepatocellular carcinoma is largely refractory to most chemotherapeutic agents (Zhu, 2006). As expected, hepatoma 22 (H22) cells subjected to NDP treatment at a pharmacological dose exhibited a drug-resistant phenotype with a prominent feature of enlarged cells equipped with an enhanced antioxidant arsenal. These profiles could be demonstrated owing to the likelihood that intact cells could be more readily isolated from ascitic fluid. Based on this model, we clearly demonstrated that BSO eliminated NDP-induced resistance. Protein levels went up at 72 h after 25 mg/kg NDP treatment (Fig. 3B) because the cells became much bigger (Fig. 2B). G2 phase prior to cell division has two prominent features; one is cell growth, another is massive syntheses of protein and RNA (Alberts et al., 2008). G2/M arrest was able to induce morphological enlargement of human leukemia HL-60 cells (Hsu et al., 2012). In the present experimental model, we observed that NDP-induced G2/M arrest caused not only morphological enlargement of H22 cells, but also the accumulation of both protein and RNA (Fig. 3B and Supplementary Fig. 1D). Since protein was a variable, the tested biological parameters were not normalized on a per milligram protein basis; rather they were normalized on the basis of per million cells. Such a normalization method has yet been commonly employed (Barranco et al., 1990, Hunter et al., 1987, Lee et al., 1989). If TrxR activity was normalized to protein content, 25 mg/kg NDP still shows TrxR inhibition by about 50% at 6 h (Fig. 3C), because cell volume was not obviously

altered (Fig. 2B) and protein levels remained the same as the control (Fig. 3B). However, if TrxR activity was normalized to protein content, the TrxR activity was almost the same as the control at 72 h, no longer exhibiting the 3-fold increase as seen in Fig. 3C, where TrxR was normalized to cell counts. Overall, the TrxR activity at 72 h indicates that NDP does not provide long-term inhibition of TrxR activity, *i.e.* TrxR activity is able to recover back to normal levels on the basis of protein amounts or increases to a level significantly higher than normal level on the basis of cell counts, provided that cells become bigger. Such a seemingly peculiar phenomenon, referred to as temporal inactivation of TrxR activity, is actually not unprecedented in animal studies; in fact, this adaptive response in tumor and normal tissues in mice has been well demonstrated. For example, TrxR activity can recover back to normal levels at 48–72 h after being significantly inhibited by cyclophosphamide, ifosfamide and cisplatin at 4–6 h post administration of these drugs at pharmacological levels (Wang et al., 2007, Wang et al., 2008, Zhang and Lu, 2007, Zhang et al., 2008). In this regard, the present results obtained using NDP are quite consistent with the findings of previous studies of mechanistically similar chemotherapeutic drugs in mice. Resistance to chemotherapy severely limits its effectiveness (Gottesman and Pastan, 1988). The survival of cancer cells after attack by chemotherapeutic drugs may lead to the emergence of drug resistance (Stordal and Davey, 2007). At 72 h after 25 mg/kg NDP treatment, the proliferation of H22 cells was fully inhibited relative to the cell numbers counted at 6 h (290 *versus* 293 million), whereas H22 cells without NDP treatment proliferated from about 300 million at 6 h to roughly 1800 million at 72 h (Fig. 3A). The NDP-generated proliferation-compromised viable cells displayed an enlarged morphology (Fig. 2B). Accordingly, NPFT levels and activities of a number of antioxidant enzymes substantially increased, on the basis of the same amount of cells (Figs. 3C, D, 5D). This expanded antioxidant arsenal, as an adaptive response, may help the ascitic H22 cells increase their resistance to further drug treatments. Additionally, we used qRT-PCR and western blot methods to characterize the gene and protein expression of TrxR1, and the results achieved are consistent with our previous finding of TrxR activity, namely, that NDP at 72 h increased TrxR activity *via* elevating the mRNA and protein of TrxR1 (Supplementary Fig. 1).

GSH, a major component of NPFT, plays a crucial role in cell defense mechanisms by acting as an antioxidant and conjugating with toxic electrophiles (Davis et al., 2001, Lu et al., 2007). The GSH system, comprising NADPH, GSH and GR coupled with glutaredoxins, provides electrons to ribonucleotide reductase (RNR) for DNA synthesis (Holmgren, 1989, Lu et al., 2007). GSH also participates in providing electrons to GPxs for scavenging hydrogen peroxide (Brigelius-Flohé and Kipp, 2009, Steinbrenner and Sies, 2009). The Trx system, composed of NADPH, Trx and TrxR, is a crucial electron donor system to RNR for DNA synthesis (Holmgren, 1989, Lu et al., 2007). Trx also provides electrons to peroxiredoxin for removing hydrogen peroxide (Hall et al., 2011, Thamsen et al., 2011). Therefore, compared to TrxR inhibition alone, the inhibition of both the Trx and GSH systems attenuates the detoxification of electrophilic xenobiotics and enhances DNA synthesis inhibition and oxidative stress. Hence, the simultaneous inhibition of both the Trx and GSH systems is a more powerful strategy for cancer control, given that the host could be tolerant to the co-treatment of TrxR and GSH synthesis inhibitors. In cultured cancer cells, GSH depletion by BSO potentiates the cytotoxicity of arsenic trioxide, a TrxR inhibitor (Lu et al., 2007). In the present study, we showed BSO *per se* neither had cytotoxicity nor caused host toxicity except that it significantly suppressed NPFT levels in H22 cells and renal tissues. However, BSO effectively prevented NDP-induced enlargement of cellular morphology

(Fig. 4C), as well as the elevation of antioxidant arsenal (Fig. 5D). The combination of BSO and NDP was more cytotoxic than NDP alone to ascitic H22 cells since the combination treatment decimated the cell population to less than 30 million, whereas viable cells in treated with NDP alone still remained at a level of roughly 300 million (Fig. 5B), being equipped with increased antioxidant arsenal as compared with the cells in the combination treatment (Fig. 5D). It is worth noting that mice had no apparent difficulties tolerating treatment with either NDP alone or the combination of BSO and NDP, no symptoms of toxicity were observed during the experimental period. Therefore, herein we have provided *in vivo* evidence that simultaneous modulation of TrxR and GSH is indeed more effective in coping with cancer cells than single modulation of TrxR, without an increase in host toxicity. Moreover, an *in vitro* experiment using human oral squamous cell carcinoma cell line Tca8113 was performed. As shown in Supplementary Fig. 2, at 6 h we found NDP inhibited TrxR activity and BSO suppressed NPFT levels, both in a dose-associated fashion. Furthermore, at 18 h, the combination of NDP and BSO enhanced cytotoxicity compared to NDP alone, whereas BSO itself did not cause cell death.

BSO not only inhibits GSH synthesis in cancer cells, it also suppresses GSH levels of normal tissues. Ifosfamide and cisplatin not only inhibit tumor TrxR activity, they also efficiently suppress renal TrxR activity (Zhang and Lu, 2007, Zhang et al., 2008). Although the simultaneous modulation of TrxR and GSH appears to be a powerful strategy for cancer therapy, the combination of BSO with either ifosfamide or cisplatin has an obvious drawback, because kidney tissue cannot escape from the simultaneous modulation. Indeed, either ifosfamide- or cisplatin-generated nephrotoxicity could be largely aggravated by BSO treatments (Satoh et al., 2000, Zhang and Lu, 2007). As an analogue of cisplatin, NDP is less potent than cisplatin in generating nephrotoxicity at concentrations where both agents display equivalent anticancer activity, whereas the dose-limiting toxicity of NDP is myelosuppression, in particular thrombocytopenia (Desoize and Madoulet, 2002, Kawai et al., 2005, Ogawa, 1996, Sasaki et al., 1991, Vermorken, 2001). A recent study indicated that BSO and TrxR inhibitor auranofin potentiate 17-allylamino-17-demethoxygeldanamycin induced cancer cell killing (Scarbrough et al., 2012), and mice treated simultaneously with BSO and auranofin showed no alterations in circulating leukocytes or red blood cells (Fath et al., 2011), thus suggesting that the combination of TrxR and GSH does not aggravate myelosuppression. Consistent with this conclusion, the present study demonstrates that the combination of NDP and BSO does not generate significant hematological toxicity (Fig. 6E). TrxR inhibition is known to largely underlie ifosfamide- or cisplatin-generated nephrotoxicity (Zhang and Lu, 2007, Zhang et al., 2008); herein, we have shown that NDP at the pharmacological level used does not inhibit renal TrxR activity (Fig. 6A); accordingly, renal tissues were not subjected to the simultaneous modulation of TrxR and GSH (Figs. 6A, B), and as a result, renal structures as well as plasma BUN and Cr all remained normal (Figs. 6D, E), which is consistent with the observation that NDP-induced growth suppression was not enhanced by BSO (Fig. 6C).

In conclusion, the present study has revealed that the anticancer mechanism of NDP involves TrxR inhibition, and that as an adaptive response to this inhibition, the viable ascitic cancer cells after NDP treatment enlarge themselves to expand their intracellular antioxidant arsenal. Furthermore, BSO is a powerful agent that can eliminate this GSH-dependent adaptive response and thus enhance the therapeutic efficacy of NDP.

Disclosure of potential conflicts of interest

No potential conflicts of interest were disclosed.

Acknowledgments

The authors thank Prof. Jun Li (School of Pharmacy, Anhui Medical University) for technical assistance. This study was supported by National Natural Science Foundation (31170648 to Zhang J), a grant from Anhui Agricultural University to Zhang J, and a grant from Department of Education of Anhui Province (2011SQRL051 to Wang Y).

References

Alberto, M.E., Lucas, M.F., Pavelka, M., Russo, N., 2009. The second-generation anticancer drug nedaplatin: a theoretical investigation on the hydrolysis mechanism. J. Phys. Chem. B 113, 14473–14479.

Alberts, B., Johnson, A., Lewis, J., Raff, M., Roberts, K., Walter, P., 2008. Molecular Biology of the Cell, 5th edition. Garland Science, New York.

Andringa, K.K., Coleman, M.C., Aykin-Burns, N., Hitchler, M.J., Walsh, S.A., Domann, E.E., Spitz, D.R., 2006. Inhibition of glutamate cysteine ligase activity sensitizes human breast cancer cells to the toxicity of 2-deoxy-D-glucose. Cancer Res. 66, 1605–1610.

Anestål, K., Arnér, E.S., 2003. Rapid induction of cell death by selenium-compromised thioredoxin reductase 1 but not by the fully active enzyme containing selenocysteine. J. Biol. Chem. 278, 15966–15972.

Anestål, K., Prast-Nielsen, S., Cenas, N., Arnér, E.S., 2008. Cell death by SecTRAPs: thioredoxin reductase as a prooxidant killer of cells. PLoS One 3, e1846.

Arnér, E.S., 2009. Focus on mammalian thioredoxin reductases — important selenoproteins with versatile functions. Biochim. Biophys. Acta 1790, 495–526.

Barranco, S.C., Townsend Jr., C.M., Weintraub, B., Beasley, E.G., MacLean, K.K., Shaeffer, J., Liu, N.H., Schellenberg, K., 1990. Changes in glutathione content and resistance to anticancer agents in human stomach cancer cells induced by treatments with melphalan in vitro. Cancer Res. 50, 3614–3618.

Biroccio, A., Benassi, B., Fiorentino, F., Zupi, G., 2004. Glutathione depletion induced by c-Myc downregulation triggers apoptosis on treatment with alkylating agents. Neoplasia 6, 195–206.

Brigelius-Flohé, R., Kipp, A., 2009. Glutathione peroxidases in different stages of carcinogenesis. Biochim. Biophys. Acta 1790, 1555–1568.

Cai,W., Zhang, L., Song, Y.,Wang, B., Zhang, B., Cui, X., Hu, G., Liu, Y.,Wu, J., Fang, J., 2012a. Small molecule inhibitors of mammalian thioredoxin reductase. Free Radic. Biol. Med. 52, 257–265.

Cai, W., Zhang, B., Duan, D., Wu, J., Fang, J., 2012b. Curcumin targeting the thioredoxin system to elevate oxidative stress in HeLa cells. Toxicol. Appl. Pharmacol. [Epub ahead of print].

Carlberg, I.,Mannervik, B., 1985. Glutathione reductase. Methods Enzymol. 113, 484–490.

Dai, J., Weinberg, R.S., Waxman, S., Jing, Y., 1999. Malignant cells can be sensitized to undergo growth inhibition and apoptosis by arsenic trioxide through modulation of the glutathione redox system. Blood 93, 268–277.

Davis Jr., W., Ronai, Z., Tew, K.D., 2001. Cellular thiols and reactive oxygen species in drug-induced apoptosis. J. Pharmacol. Exp. Ther. 296, 1–6.

Desoize, B.,Madoulet, C., 2002. Particular aspects of platinum compounds used at present in cancer treatment. Crit. Rev. Oncol. Hematol. 42, 317–325.

Fath, M., Ahmad, I.M., Smith, C.J., Spence, J.M., Spitz, D.R., 2011. Enhancement of carboplatin-mediated lung cancer cell killing by simultaneous disruption of glutathione and thioredoxin metabolism. Clin. Cancer Res. 17, 6206–6217.

Gladyshev, V.N., Jeang, K.T., Stadtman, T.C., 1996. Selenocysteine, identified as the penultimate C-terminal residue in human T-cell thioredoxin reductase, corresponds to TGA in the human placental gene. Proc. Natl. Acad. Sci. U. S. A. 93, 6146–6151.

Gottesman, M.M., Pastan, I., 1988. Resistance to multiple chemotherapeutic agents in human cancer cells. Trends Pharmacol. Sci. 9, 54–58.

Gromer, S., Urig, S., Becker, K., 2004. The thioredoxin system — from science to clinic. Med. Res. Rev. 24, 40–89.

Habig, W.H., Pabst, M.J., Jakoby, W.B., 1974. Glutathione S-transferases: the first enzymatic step in mercapturic acid formation. J. Biol. Chem. 249, 7130–7139.

Hall, A., Nelson, K., Poole, L.B., Karplus, P.A., 2011. Structure-based insights into the catalytic power and conformational dexterity of peroxiredoxins. Antioxid. Redox Signal. 15, 795–815.

Holmgren, A., 1989. Thioredoxin and glutaredoxin systems. J. Biol. Chem. 264, 13963–13966.

Holmgren, A., Björnstedt, M., 1995. Thioredoxin and thioredoxin reductase. Methods Enzymol. 252, 199–208.

Hsu, M.H., Liu, C.Y., Lin, C.M., Chen, Y.J., Chen, C.J., Lin, Y.F., Huang, L.J., Lee, K.H., Kuo, S.C., 2012. 2-(3-Methoxyphenyl)-5-methyl-1,8-naphthyridin-4(1H)-one (HKL-1) induces G2/M arrest and mitotic catastrophe in human leukemia HL-60 cells. Toxicol. Appl. Pharmacol. 259, 219–226.

Hunter, K.J., Deen, D.F., Marton, L.J., 1987. Changes in the glutathione content of rat 9L cells induced by treatment with the ornithine decarboxylase inhibitor alphadifluoromethylornithine. Cancer Res. 47, 5270–5273.

Kawai, Y., Taniuchi, S., Okahara, S., Nakamura, M., Gemba, M., 2005. Relationship between cisplatin or nedaplatin-induced nephrotoxicity and renal accumulation. Biol. Pharm. Bull. 28, 1385–1388.

Koshiyama, M., Kinezaki, M., Uchida, T., Sumitomo, M., 2005. Chemosensitivity testing of a novel platinum analog, nedaplatin (254-S), in human gynecological carcinomas: a comparison with cisplatin. Anticancer Res. 25, 4499–4502.

Lee, F.Y., Vessey, A., Rofstad, E., Siemann, D.W., Sutherland, R.M., 1989. Heterogeneity of glutathione content in human ovarian cancer. Cancer Res. 49, 5244–5248.

Lu, J., Chew, E.H., Holmgren, A., 2007. Targeting thioredoxin reductase is a basis for cancer therapy by arsenic trioxide. Proc. Natl. Acad. Sci. U. S. A. 104, 12288–12293.

Meurette, O., Lefeuvre-Orfila, L., Rebillard, A., Lagadic-Gossmann, D., Dimanche-Boitrel, M.T., 2005. Role of intracellular glutathione in cell sensitivity to the apoptosis induced by tumor necrosis factor {alpha}-related apoptosis-inducing ligand/anticancer drug combinations. Clin. Cancer Res. 11, 3075–3083.

Monk, B.J., Alberts, D.S., Burger, R.A., Fanta, P.T., Hallum III, A.V., Hatch, K.D., Salmon, S.E., 1998. In vitro phase II comparison of the cytotoxicity of a novel platinum analog, nedaplatin (254-S), with that of cisplatin and carboplatin against fresh, human cervical cancers. Gynecol. Oncol. 71, 308–312.

Nguyen, P., Awwad, R.T., Smart, D.D., Spitz, D.R., Gius, D., 2006. Thioredoxin reductase as a novel molecular target for cancer therapy. Cancer Lett. 236, 164–174.

Nordberg, J., Arnér, E.S., 2001. Reactive oxygen species, antioxidants, and the mammalian thioredoxin system. Free Radic. Biol. Med. 31, 1287–1312.

Ogawa, M., 1996. 254-S, NK121 and TRK710. In: Pinedo, H.M., Schornagel, J.H. (Eds.), Plenum Press, New York, pp. 193–197.

Pennington, J.D., Jacobs, K.M., Sun, L., Bar-Sela, G., Mishra, M., Gius, D., 2007. Thioredoxin and thioredoxin reductase as redox-sensitive molecular targets for cancer therapy. Curr. Pharm. Des. 13, 3368–3377.

Rotruck, J.T., Pope, A.L., Ganther, H.E., Swanson, A.B., Hafeman, D.G., Hoekstra,W.G., 1973. Selenium: biochemical role as a component of glutathione peroxidase. Science 179, 588–590.

Saitoh, M., Nishitoh, H., Fujii, M., Takeda, K., Tobiume, K., Sawada, Y., Kawabata, M., Miyazono, K., Ichijo, H., 1998. Mammalian thioredoxin is a direct inhibitor of apoptosis signal-regulating kinase (ASK) 1. EMBO J. 17, 2596–2606.

Sasaki, Y., Amano, T., Morita,M., Shinkai, T., Eguchi, K., Tamura, T.,Ohe, Y., Kojima, A., Saijo, N., 1991. Phase I study and pharmacological analysis of cis-diammine(glycolato) platinum (254-S; NSC 375101D) administered by 5-day continuous intravenous infusion. Cancer Res. 51, 1472–1477.

Satoh, M., Shimada, A., Zhang, B., Tohyama, C., 2000. Renal toxicity caused by cisplatinum in glutathione-depleted metallothionein-null mice. Biochem. Pharmacol. 60, 1729–1734.

Scarbrough, P.M., Mapuskar, K.A., Mattson, D.M., Gius, D., Watson, W.H., Spitz, D.R., 2012. Simultaneous inhibition of glutathione- and thioredoxin-dependent metabolism is necessary to potentiate 17AAG-induced cancer cell killing via oxidative stress. Free Radic. Biol. Med. 52, 436–443.

Steinbrenner, H., Sies, H., 2009. Protection against reactive oxygen species by selenoproteins. Biochim. Biophys. Acta 1790, 1478–1485.

Stordal, B., Davey, M., 2007. Understanding cisplatin resistance using cellular models. IUBMB Life 59, 696–699.

Sun, Y., Oberley, L.W., Li, Y., 1988. A simple method for clinical assay of superoxide dismutase. Clin. Chem. 34, 497–500.

Thamsen, M., Kumsta, C., Li, F., Jakob, U., 2011. Is overoxidation of peroxiredoxin physiologically significant? Antioxid. Redox Signal. 14, 725–730.

Tonissen, K.F., Di Trapani, G., 2009. Thioredoxin system inhibitors as mediators of apoptosis for cancer therapy. Mol. Nutr. Food Res. 53, 87–103.

Troyano, A., Fernández, C., Sancho, P., de Blas, E., Aller, P., 2001. Effect of glutathione depletion on antitumor drug toxicity (apoptosis and necrosis) in U-937 human promonocytic cells. The role of intracellular oxidation. J. Biol. Chem. 276, 47107–47115.

Vermorken, J.B., 2001. The integration of paclitaxel and new platinum compounds in the treatment of advanced ovarian cancer. Int. J. Gynecol. Cancer 11 (Suppl.), 121–130.

Wang, X., Zhang, J., Xu, T., 2007. Cyclophosphamide as a potent inhibitor of tumor thioredoxin reductase in vivo. Toxicol. Appl. Pharmacol. 218, 88–95.

Wang, X., Zhang, J., Xu, T., 2008. Thioredoxin reductase inactivation as a pivotal mechanism of ifosfamide in cancer therapy. Eur. J. Pharmacol. 579, 66–73.

Witte, A.B., Anestål, K., Jerremalm, E., Ehrsson, H., Arnér, E.S., 2005. Inhibition of thioredoxin reductase but not of glutathione reductase by the major classes of alkylating and platinum-containing anticancer compounds. Free Radic. Biol. Med. 39, 696–703.

Wu, X.X., Ogawa, O., Kakehi, Y., 2004. Enhancement of arsenic trioxide-induced apoptosis in renal cell carcinoma cells by L-buthionine sulfoximine. Int. J. Oncol. 24, 1489–1497.

Yoo, M.H., Xu, X.M., Carlson, B.A., Gladyshev, V.N., Hatfield, D.L., 2006. Thioredoxin reductase 1 deficiency reverses tumor phenotype and tumorigenicity of lung carcinoma cells. J. Biol. Chem. 281, 13005–13008.

Zhang, J., Lu, H., 2007. Ifosfamide induces acute renal failure via inhibition of the thioredoxin reductase activity. Free Radic. Biol. Med. 43, 1574–1583.

Zhang, J., Wang, X., Lu, H., 2008. Amifostine increases cure rate of cisplatin on ascites hepatoma 22 via selectively protecting renal thioredoxin reductase. Cancer Lett. 260, 127–136.

Zhu, A.X., 2006. Systemic therapy of advanced hepatocellular carcinoma: how hopeful should we be? Oncologist 11, 790–800.

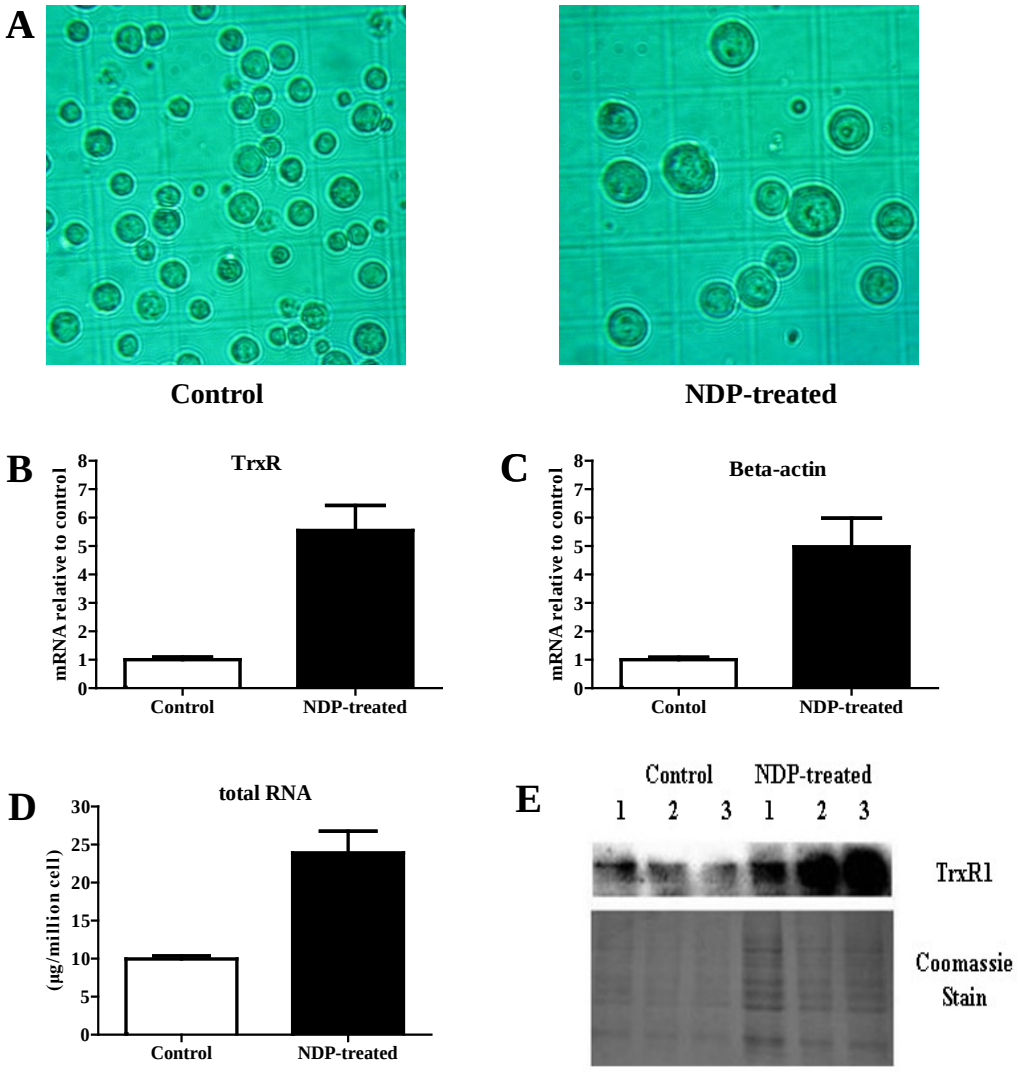

Supplementary Fig. 1. Effects of NDP on TrxR expression in ascitic H22 cells. Mice were i.p. injected with saline or 25 mg/kg NDP at 72 h after H22 cells were inoculated, then sacrificed at 144 h. mRNA levels were analyzed by real-time PCR, followed the instructions of the RT-PCR PrimerScript RT reagent Kit (TaKaRa) using the Bio-Rad CFX Manager Detection System, Forward primer of TrxR1: 5'-ACCTGGGCATCCCTGGAGAC-3'. Reverse primer of TrxR1: 5'-GCACCATTACAGTGACGTCTAAGC-3'. Forward primer of Beta-actin: 5'-GCTGAGAGGGAAATCGTGCGT-3'. Reverse primer of Beta-actin: 5'-ACCGCTCGTTGCCAATAGTGA-3'. RT-PCR conditions: 95℃ for 30s, then 35 cycles at 95℃ for 5 s，56℃ for 30 s and 72℃ for 30 s. Data were shown as relative to equivalent amounts of cells. (A) Cellular morphology (×200). Cells were observed under an optical microscope. (B) mRNA levels of TrxR1. (C) mRNA levels of Beta-actin. (D) Total RNA levels. Data in B, C and D are expressed as mean ± SEM (n = 6). (E) Western blot analysis of TrxR1. TrxR1 antibody was purchased from Santa Cruz. Protein extracts were prepared from ascitic H22 cells; representative results of three independent experiments are shown. Coomassie blue staining is shown in the bottom panel.

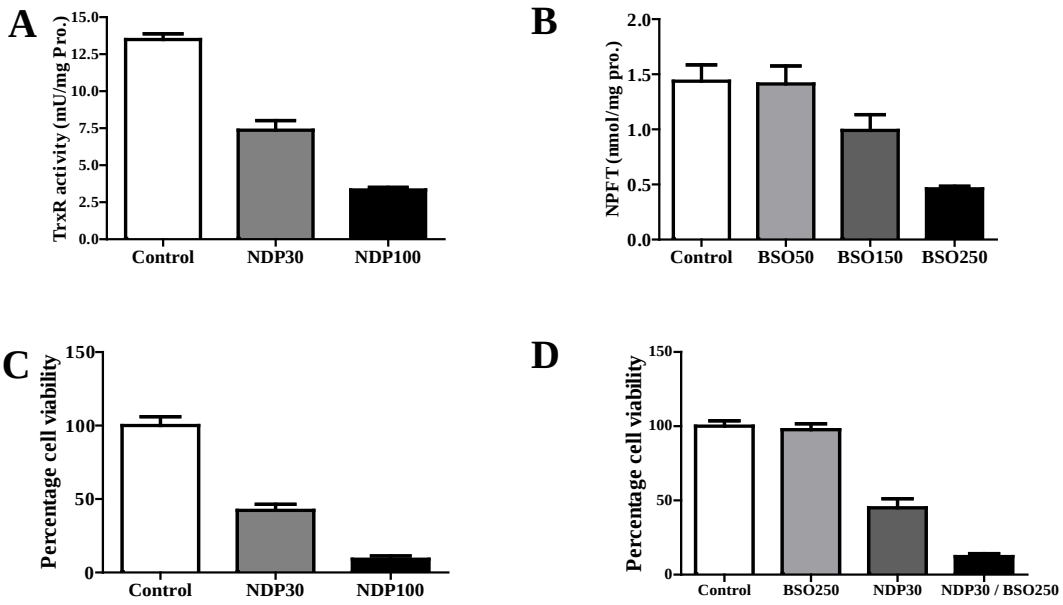

Supplementary Fig. 2. Impact of BSO on the effect of NDP in oral squamous cell carcinoma Tca8113 *in vitro*. Tca8113 Cells purchased from Cell Bank of the Chinese Academy of Sciences were cultured in RPMI1640 media containing 10% fetal calf serum (Hyclone), incubated at 37ºC, 5% CO_2 for 72 h, and cells were treated with NDP (μg/ml) or NDP plus BSO (μM). Viable cell number was determined as described in materials and methods. (A) Dose effect of NDP on TrxR activity at 6 h. (B) Dose effect of NDP on NPFT levels at 6 h. (C) Cytotoxic effect of NDP at 18 h. (D) Cytotoxic effect of NDP or BSO alone and NDP plus BSO at 18 h. Data in B, C and D are expressed as mean ± SEM (n = 3).